

The Central kpc of Starbursts and AGN
ASP Conference Series, Vol. xxx, 2001
J. H. Knapen, J. E. Beckman, I. Shlosman, and T. J. Mahoney

The $[\text{O III}]\lambda 4363$ Emitting Region Obscured by Dusty Tori

Tohru NAGAO, Takashi MURAYAMA, and Yoshiaki TANIGUCHI

*Astronomical Institute, Graduate School of Science, Tohoku University,
Aramaki, Aoba, Sendai 980-8578, Japan*

Abstract. The emission-line flux ratio of $[\text{O III}]\lambda 4363/[\text{O III}]\lambda 5007$ is a useful diagnostic for the ionization mechanism and physical properties of narrow-line regions in active galactic nuclei. However, it is known that simple photoionization models underpredict this ratio. In this contribution, we report on some pieces of evidence that a large fraction of the $[\text{O III}]\lambda 4363$ emission arises from the dense gas, which can be obscured by dusty tori. Taking this dense component into account, we show that the flux ratio of $[\text{O III}]\lambda 4363/[\text{O III}]\lambda 5007$ can be explained by two-component photoionization models.

1. Introduction

It has often been considered that the narrow-line regions (NLRs) in active galactic nuclei (AGNs) are photoionized by the radiation from central engines. However, this photoionization scenario has sometimes been conflicted with several serious problems. One of such problems is that any single-zone photoionization models underpredict the $[\text{O III}]\lambda 4363/[\text{O III}]\lambda 5007$ flux ratio, R_{OIII} (e.g., Simpson et al. 1996). To solve this problem, some models have been proposed; e.g., two component models with high-density gas clouds (e.g., Filippenko 1985) or those with shock-heated regions (e.g., Dopita & Sutherland 1995). In addition, some previous studies reported that type 1 and type 1.5 Seyfert nuclei (S1s and S1.5s, respectively) tend to have higher R_{OIII} values than type 2 Seyfert nuclei (S2s) (e.g., Heckman & Balick 1979).

In order to know where and how the $[\text{O III}]\lambda 4363$ emission is radiated, and in order to solve the underprediction problem of R_{OIII} , it seems critically important to investigate why S1s show higher R_{OIII} than S2s. Therefore, we examine how the observed value of R_{OIII} depends on the AGN type based on a large sample of AGNs compiled from the literature. Then, we compare R_{OIII} with various parameters to know the nature of the $[\text{O III}]\lambda 4363$ emitting regions in AGNs (see Nagao, Murayama, & Taniguchi 2001 for more details).

2. Results

In order to investigate statistical properties of R_{OIII} , we compiled R_{OIII} of 82 S1s, 54 S1.5s, and 78 S2s, from the literature. The histograms of R_{OIII} for each Seyfert type are shown in Figure 1. It is clearly shown that the S2s exhibit

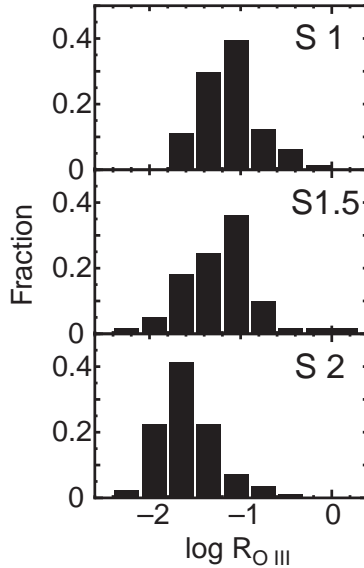


Figure 1. Frequency distributions of R_{OIII} for the S1s, the S1.5s, and the S2s.

lower R_{OIII} than the S1s and the S1.5s. According to the Kolmogorov-Smirnov statistical test, the probability which the distribution of R_{OIII} of S2s and that of S1s or S1.5s come from the same underlying population is less than 10^{-6} .

To explore the origin of this AGN-type dependence of R_{OIII} and the nature of the $[\text{O III}]\lambda 4363$ emitting regions, we compare R_{OIII} with various parameters. The results are as follows:

- *The higher- R_{OIII} objects show the hotter mid-infrared (MIR) colors.* The hotter MIR colors are thought to be attributed to the hotter dusty grains located at the inner surface of the dusty tori, which can be seen if we see the torus from a favored viewing angle (i.e., a nearly face-on view). Therefore, this means that the higher- R_{OIII} objects are seen from a more face-on view toward dusty tori than the lower- R_{OIII} objects.
- *The higher- R_{OIII} objects show the stronger $[\text{Fe VII}]\lambda 6087$ and $[\text{Fe X}]\lambda 6374$ emission.* Since a large fraction of high-ionization emission lines is thought to arise from dense gas clouds obscured by the dusty tori (e.g., Murayama & Taniguchi 1998a), the higher- R_{OIII} can be attributed to the significant flux contribution from such a high-density gas cloud.
- *The higher- R_{OIII} objects tend to show the larger $\text{FWHM}([\text{O III}]\lambda 4363)/\text{FWHM}([\text{O III}]\lambda 5007)$ ratios.* This also suggests that the $[\text{O III}]\lambda 4363$ emitting regions are located at inner regions compared to the $[\text{O III}]\lambda 5007$ emitting regions.
- *The S1s have wider $\text{FWHM}([\text{O III}]\lambda 4363)$ and larger ratio of $\text{FWHM}([\text{O III}]\lambda 4363)/\text{FWHM}([\text{O III}]\lambda 5007)$ than the S2s.* This suggests that the [O

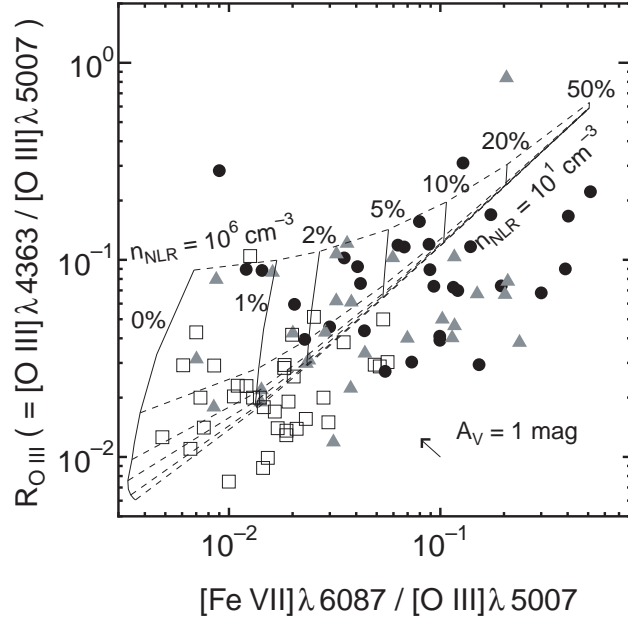


Figure 2. Diagram of R_{OIII} vs. $[\text{Fe VII}]\lambda 6087 / [\text{O III}]\lambda 5007$. The data of the S1s, the S1.5s, and the S2s are shown by filled circles, gray triangles, and open squares, respectively. Loci of our model calculations are superposed in the figure. The fraction of the flux contribution from the dense component into the $[\text{O III}]\lambda 5007$ emission is shown (0%, 1%, ..., 50%). The data points will move on the diagram as shown by the arrow if the extinction correction of $A_V = 1.0$ mag is applied.

$[\text{O III}]\lambda 4363$ emitting regions are located at inner regions compared to the $[\text{O III}]\lambda 5007$ emitting regions and have an anisotropic property.

All of these facts can be consistently understood when we introduce the high-density gas clouds located close to the nucleus, which emit a large fraction of the $[\text{O III}]\lambda 4363$ emission. Since these clouds may suffer significantly from the obscuration by dusty tori in S2s, we conclude that the AGN-type dependence of R_{OIII} is attributed to the viewing-angle dependence of the visibility of the high-density gas clouds.

3. Discussion

To examine whether or not the viewing-angle dependence of the visibility of the high-density gas can account for the observed difference in R_{OIII} between S1s and S2s in the framework of the photoionization scheme, we carry out dual-component photoionization model calculations following the manner of Murayama & Taniguchi (1998b). This method takes account of such high-density gas clouds as a strong $[\text{O III}]\lambda 4363$ emitter, in addition to the typical NLR component.

We perform model calculations using the spectral synthesis code *Cloudy* version 90.04 (Ferland 1996). We assume uniform density gas clouds with a plane-parallel geometry. The dense component (DC) is assumed to be truncated clouds to avoid unusually strong [O I] emission. Here we assume $n_{\text{DC}} = 10^7 \text{ cm}^{-3}$. We perform several model runs covering $10^1 \text{ cm}^{-3} \leq n_{\text{NLR}} \leq 10^6 \text{ cm}^{-3}$. The ionization parameter of the NLR component is assumed as $U_{\text{NLR}} = 10^{-2}$. The ionization parameter and the hydrogen column density of DC are determined by the following two conditions: $([\text{Fe x}]/[\text{Fe VII}])_{\text{DC}} = 0.8$ and $([\text{Fe VII}]/[\text{O III}]\lambda 5007)_{\text{DC}} = 1.0$. The former ratio is the typical value of Seyfert galaxies (Nagao, Taniguchi, & Murayama 2000), and the latter condition is introduced by Murayama & Taniguchi (1998b). As a result, $U_{\text{DC}} = 10^{-1.48}$ and $N_{\text{DC}} = 10^{20.76} \text{ cm}^{-2}$ are adopted. The calculations are stopped when the gas temperature falls to 4000K for the NLR component. We set the gas-phase element abundances to be solar ones. We adopt the power-law continuum as $\alpha = -1.5$ between $10 \mu\text{m}$ and 50 keV in the form $f_{\nu} \propto \nu^{\alpha}$. The spectral index is set to $\alpha = 2.5$ at lower energy (i.e., $\lambda \geq 10 \mu\text{m}$) and to $\alpha = -2$ at higher energy (i.e., $h\nu \geq 50 \text{ keV}$). The fraction of DC to the NLR component is treated as a free parameter in our calculations.

We present our model calculations and compare them with the observations in a diagram of R_{OIII} versus $[\text{Fe VII}]/[\text{O III}]\lambda 5007$ (Figure 2). We find that the model grids are roughly consistent with the observations if we take the effects of the correction for the extinction into account. Though the dispersion of observation appears to be larger than the model grids, this may be attributed to the fact that the parameters, e.g., U_{NLR} and n_{DC} , are different from object to object. It is shown that the R_{OIII} of the S1s can be explained by introducing a 5% – 20% contribution from DC while the R_{OIII} of the S2s can be explained by introducing a 0% – 2% contribution from DC.

Through the dual-component photoionization model calculations, we conclude that (1) the origin of the AGN-type dependence of R_{OIII} is the viewing-angle dependence (i.e., the AGN-type dependence) of the visibility of the dense gas clouds which can be hidden by dusty tori, and (2) the underprediction problem of R_{OIII} is solved taking such high-density gas clouds into account.

References

Dopita, M. A., & Sutherland, R. S. 1995, ApJ, 455, 468
 Ferland, G. J. 1996, Hazy: A Brief Introduction to Cloudy (Lexington: Univ. Kentucky Dept. Phys. Astron.)
 Filippenko, A. V. 1985, ApJ, 289, 475
 Heckman, T. M., & Balick, B. 1979, A&A, 79, 350
 Murayama, T., & Taniguchi, Y. 1998a, ApJ, 497, L9
 Murayama, T., & Taniguchi, Y. 1998b, ApJ, 501, L115
 Nagao, T., Murayama, T., & Taniguchi, Y. 2001, ApJ, 549, 155
 Nagao, T., Taniguchi, Y., & Murayama, T. 2000, AJ, 119, 2605
 Simpson, C., Ward, M., Clements, D. L., & Rawlings, S. 1996, MNRAS, 281, 509